

Q-Enhancement of Microelectromechanical Filters Via Low-Velocity Spring Coupling

Kun Wang, Frank D. Bannon III, John R. Clark, and Clark T.-C. Nguyen

Center for Integrated Sensors and Circuits
Department of Electrical Engineering and Computer Science
University of Michigan

2406 EECS Bldg., 1301 Beal Ave., Ann Arbor, Michigan 48109-2122, email: ctnguyen@eecs.umich.edu

ABSTRACT

A micromechanical filter design technique based on low-velocity coupling of resonators is described that can achieve percent bandwidths less than 0.1% without the need for aggressive, submicron lithography. Using this low-velocity coupling technique, an IC process limited to feature sizes no less than 2 μm was utilized to achieve three-resonator micromechanical filters centered at 340 kHz with percent bandwidths as low as 0.1% (filter Q 's as high as 800), passband rejections up to 60 dB (the highest reported to date on the micro-scale), and insertion losses less than 1 dB. In addition, two-resonator 7.82 MHz filters were demonstrated with percent bandwidths of 0.2% and comparable insertion losses, all within an area of less than $50 \times 50 \mu\text{m}^2$.

I. INTRODUCTION

Recently demonstrated high- Q micromechanical bandpass filters with area dimensions on the order of $50 \times 50 \mu\text{m}^2$ show great potential as IC-compatible micro-scale components for use in the IF (and perhaps RF) stages of compact communication transceivers [1]. Such filters are comprised of two or more flexural-mode $\mu\text{mechanical}$ resonators (each with $Q > 10,000$) coupled by flexural-mode mechanical springs with stiffnesses that largely determine the overall filter bandwidth. To date, two-resonator $\mu\text{mechanical}$ bandpass filters have been demonstrated with frequencies up to 14.5 MHz, percent bandwidths on the order of 0.2%, and insertion losses less than 1 dB [2,3]. Higher-order three-resonator filters with frequencies near 455 kHz have also been achieved, with equally impressive insertion losses, and with more than 48 dB of passband rejection [4]. However, to achieve such performance with percent bandwidths less than 0.5%, submicron coupling beam dimensions (down to 0.6 μm) were required to realize sufficiently compliant coupling springs. Although such dimensions are achievable by many of today's production IC processes, larger dimensions are preferable for better control of absolute tolerances.

This work presents a $\mu\text{mechanical}$ filter design technique based on low-velocity coupling of resonators, capable of achieving percent bandwidths less than 0.1% without the need for aggressive, submicron lithography. The basic technique takes full advantage of the dependence of resonator stiffness on location, strategically coupling resonators at low-velocity locations, where resonator stiffness is much larger than at higher velocity points. The high resonator

stiffness at these locations then allows (for a given percent bandwidth) the use of stiffer coupling springs, which can be made larger, using less demanding lithographic technologies. Both theory and experimental verification are presented in the following sections.

II. FILTER BANDWIDTH DESIGN

Figure 1 shows the perspective view schematic of the three-resonator $\mu\text{mechanical}$ filter used for this work. As with a previous design [4], this filter features three folded-beam $\mu\text{mechanical}$ resonators, soft flexural-mode coupling beams attaching resonators at their folding trusses, differential capacitive-comb transducer inputs and outputs to suppress parasitic feedthrough, and parallel-plate electrodes for voltage-controlled tuning of resonator frequencies. As will be described, this design differs from previous versions mainly in the constituent resonators, which now allow for variation in coupling point velocity.

Because planar IC processes typically exhibit substantially better *matching* tolerances than *absolute*, the constituent resonators in $\mu\text{mechanical}$ filters are normally designed to be identical, with identical spring dimensions and resonance frequencies. For such designs, the center frequency of the overall filter is equal to the resonance frequency f_o of the resonators. The filter bandwidth is determined predominantly by the stiffness of its constituent resonators (k_r) and coupling beams (k_{sij}), which must satisfy the expression:

$$BW = \left(\frac{f_o}{k_{ij}} \right) \left(\frac{k_{sij}}{k_r} \right) \quad (1)$$

where k_{ij} is a normalized coupling coefficient found in filter cookbooks [5]. Note from (1) that filter bandwidth is not dependent on the absolute values of resonator and coupling beam stiffness; rather, their ratio k_{sij}/k_r dictates bandwidth.

As described in [4], in order to accommodate the use of identical resonators in a $\mu\text{mechanical}$ filter, the dimensions of the coupling beams must correspond to an effective quarter-wavelength of the operation frequency. Specifically, for quarter-wavelength coupling, the length L_{sij} , width W_{sij} and thickness h of a coupling beam must be chosen to simultaneously satisfy the expressions [4]

$$\cos \alpha \sinh \alpha + \sin \alpha \cosh \alpha = 0 \quad (2)$$

$$k_{sij} = \frac{EI\alpha^3 (\sin \alpha + \sinh \alpha)}{L_{sij}^3 (\cos \alpha \cosh \alpha - 1)} \quad (3)$$

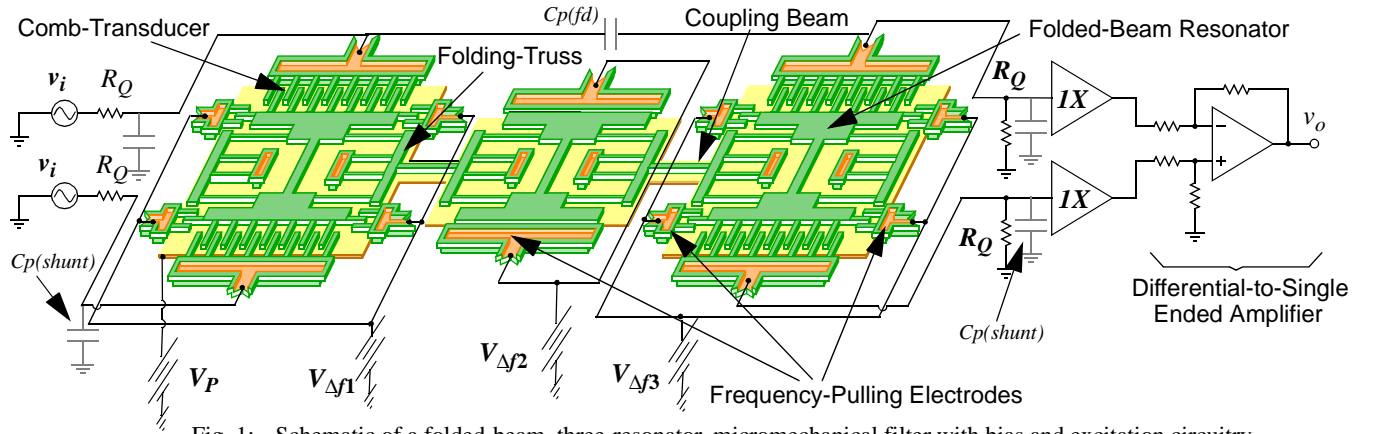


Fig. 1: Schematic of a folded-beam, three-resonator, micromechanical filter with bias and excitation circuitry.

Table I: Coupling Beam Width Requirements*

Percent BW	0.01%	0.1%	0.6%	1%
Req'd W_{sij} [μm]	0.06	0.28	1	1.32

*For a 455 kHz filter with $k_r=310$ N/m.

where $\alpha=L_{sij}(\rho A \omega_o^2/EI)^{0.25}$, $I=hW_{sij}^3/12$, and $A=W_{sij}h$. For a given value of film thickness h , and a given needed value of coupling beam stiffness k_{sij} , (2) and (3) represent two equations in two unknowns, implying that only one value of L_{sij} and one value of W_{sij} can be used to implement a given stiffness k_{sij} . If the resonator stiffness is further constrained to be constant—as was the case for the design in [4]—a scenario could arise where the unique coupling beam width W_{sij} that satisfies both quarter-wavelength and filter bandwidth requirements is a submicron dimension. Table I illustrates this problem for the case of a 455 kHz three-resonator filter with resonator stiffnesses constrained to be $k_r=310$ N/m (stiffness at the shuttle mass). Here, submicron dimensions are shown to be necessary for percent bandwidths (BW/f_o) lower than 0.67%.

III. LOW VELOCITY COUPLING

To increase the required width of a quarter-wavelength coupling beam, the value of coupling beam stiffness k_{sij} corresponding to the needed filter bandwidth BW must be increased. As indicated by Eq. (1), for a given filter bandwidth, an increase in k_{sij} is allowable only when accompanied by an equal increase in resonator stiffness k_r . Such an increase in k_r must, in turn, be accompanied by a corresponding increase in resonator mass m_r to maintain the desired filter center frequency. Thus, to maximize flexibility in attainable filter bandwidth, a convenient method for simultaneously scaling both resonator stiffness k_r and mass m_r , preferably without drastically changing overall resonator dimensions, is required.

One simple method for achieving this takes advantage of the fact that, in general, the effective dynamic stiffness and mass of a given resonator are strong functions of location on the resonator, as illustrated in Fig. 2 for a classic folded-beam micromechanical resonator. This is immediately

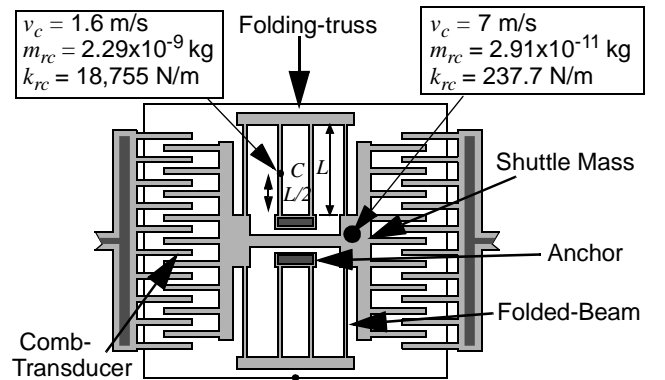


Fig. 2: Schematic of a classic folded-beam resonator, indicating mechanical impedances at certain points.

apparent with the recognition that different locations on a vibrating resonator move with different velocities, and that the dynamic mass and stiffness of a given mechanical resonator are strong functions of velocity, given by the expressions [6]

$$m_{rc} = \frac{KE_{tot}}{(1/2)v_c^2} \quad (4)$$

$$k_{rc} = \omega_o^2 m_{rc}, \quad (5)$$

where KE_{tot} is the kinetic energy, and v_c is the maximum resonance velocity at location c on the resonator. As a result, the dynamic resonator mass and stiffness “seen” by a coupling beam is a strong function of the coupling location. Fundamental-mode folded-beam resonators coupled at their shuttle masses, where the velocity is maximum, present the smallest stiffness to the coupling beam. Conversely, fundamental-mode resonators coupled at locations closer to their anchors, where velocities are many times smaller, present very large dynamic stiffnesses to their respective coupling beams, allowing much smaller percent bandwidth filters for the same coupling beam stiffnesses.

To conveniently implement low velocity coupling without substantial resonator design changes, and retaining coupling at resonator folding trusses, the folded-beam resonators used in Fig. 1 feature ratioed folded-beam lengths, as

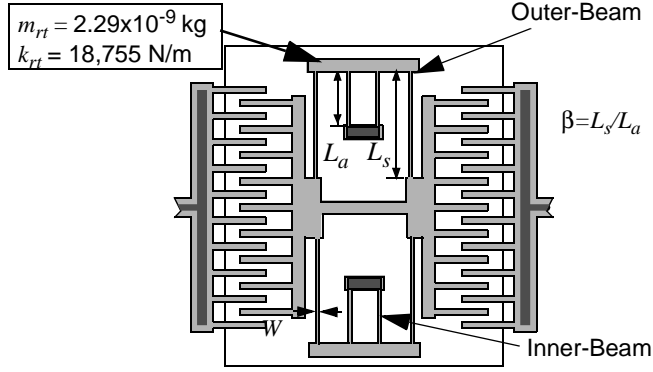


Fig. 3: Schematic of a ratioed folded-beam μ resonator for low-velocity coupling applications.

shown in Fig. 3. With this design, the maximum resonance velocity of the folding truss can be varied according to

$$v_{rt} = \frac{\omega_o X_o}{1 + \beta^3} \quad (6)$$

where ω_o is the filter center frequency, X_o is the maximum displacement at the shuttle mass, and β is the ratio of the outer beam length L_s to inner beam length L_a . Using (3) and (4), the effective dynamic stiffness k_{rt} and mass m_{rt} seen at the resonator folding trusses can be expressed as

$$k_{rt} = k_{ri}(1 + \beta^3)^2 \quad (8)$$

$$m_{rt} = m_{ri}(1 + \beta^3)^2 \quad (9)$$

where k_{ri} and m_{ri} are the effective dynamic stiffness and mass, respectively, at the resonator shuttle (maximum velocity point), given by

$$k_{ri} = \omega_o^2 m_{ri} \quad (10)$$

$$m_{ri} = M_p + \frac{M_t}{(1 + \beta^3)^2} + \frac{13}{35(1 + \beta^3)^2} M_{ba} + \left[\frac{1}{(1 + \beta^3)} + \frac{13\beta^6}{35(1 + \beta^3)^2} \right] M_{bs} \quad (11)$$

$$\omega_o = \left[\frac{4Eh(W/L_a)^3}{(1 + \beta^3)m_{ri}} \right]^{1/2} \quad (12)$$

where E is the Young's modulus; M_p is the mass of the shuttle; M_r , M_{ba} , and M_{bs} are the total folding truss, inner beam, and outer beam masses, respectively; and dimensions are defined in Fig. 3.

Figure 4 plots the dynamic stiffness (normalized against effective stiffness at the shuttle mass) at the folding truss versus β , showing a full six orders of magnitude variation in stiffness for β 's from 1 to 10. For a 360 kHz filter with 2 μ m-width coupling beams, the stiffness variation shown in Fig. 4 corresponds to a range of percent bandwidths from 0.69% to 3×10^{-6} %.

Low Velocity Coupling in HF Filters.

As explained in [2], given the general expression for mechanical resonance frequency $\omega_o = (k_r/m_r)^{0.5}$, high frequency filters require resonators with much smaller mass.

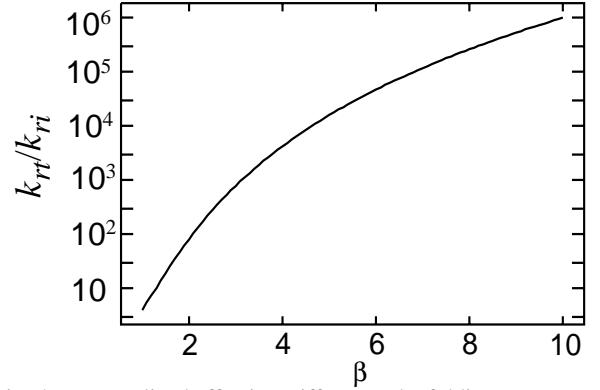


Fig. 4: Normalized effective stiffness at the folding-truss versus folded-beam ratio β .

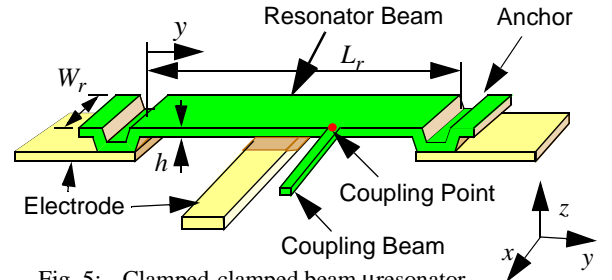


Fig. 5: Clamped-clamped beam μ resonator.

As a result, the folded-beam resonators used in the filter of Fig. 1 are inappropriate for HF or higher frequencies. Rather, clamped-clamped beam resonators, such as shown in Fig. 5, are more appropriate.

For clamped-clamped beam resonators, low velocity coupling is very easily achieved by merely moving the coupling location away from the center of the beam, as shown in Fig. 5. Using a procedure similar to that used to obtain (8) and (9), expressions for dynamic stiffness and mass as a function of distance y from the anchor are derived to be

$$k_r(y) = \omega_o^2 m_r(y) \quad (13)$$

$$m_r(y) = \frac{\rho W_r h \int_0^{L_r} [X(y')]^2 dy'}{[X(y)]^2}, \quad (14)$$

where

$$X(y) = (\cos ky - \cosh ky) - \sigma_n (\sin ky - \sinh ky) \quad (15)$$

and where ρ is the density of the structure material, $k = 4.73/L_r$, $\sigma_n = 0.9825$ for the fundamental mode, and dimensions are indicated in Fig. 5.

Figure 6 plots stiffness (normalized against the stiffness at the center of the resonator beam) versus normalized distance from an anchor for an ideal clamped-clamped beam resonator, indicating a six order of magnitude variation in stiffness for coupling locations $L_r/10$ to $L_r/2$ distant from the anchor. For a 10 MHz filter using 2 μ m-wide coupling beams, this corresponds to a range of percent bandwidths from 0.33% to 24%.

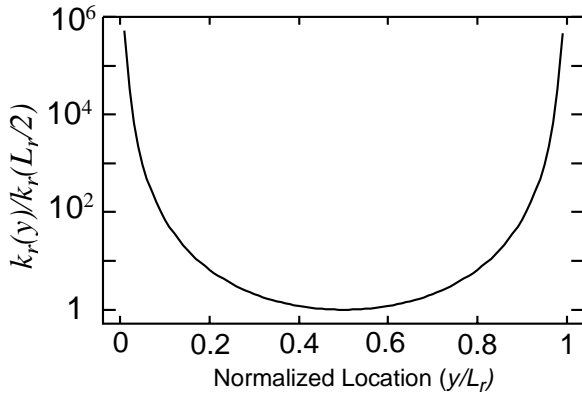


Fig. 6: Normalized effective stiffness versus normalized location on the resonator beam.

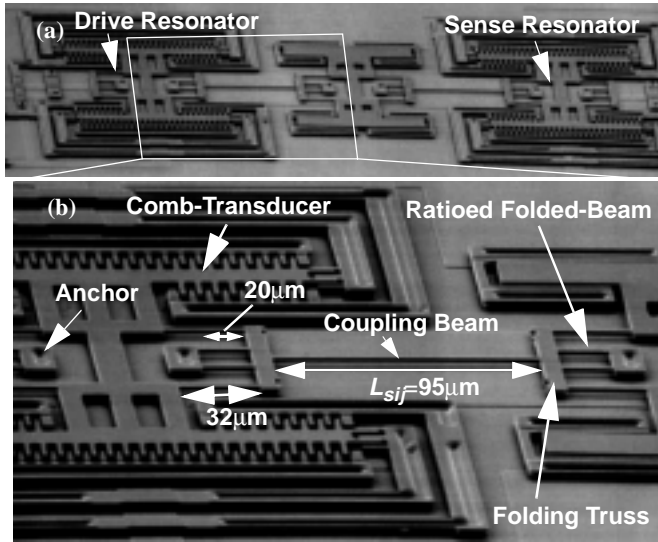


Fig. 7: SEM's of a fabricated ratioed folded-beam micromechanical filter. (a) Full view. (b) Enlarged partial view.

IV. EXPERIMENTAL RESULTS

To verify the above formulations, MF and HF μ -mechanical filters using the resonator designs of Figs. 3 and 5, respectively, were fabricated using a polysilicon surface micromachining technology [7]. Figures 7 and 8 present scanning electron micrographs (SEM's) of the completed structures, with pointers to major components. The use of low velocity coupling strategies—ratioed folded-beams in the resonators of the MF filter and coupling locations close to the anchors in the HF filter—are clearly seen in the SEM's. Design data for each of these filters are summarized in Table II.

An HP4195A Network/Spectrum Analyzer was used with a custom-built vacuum chamber [2,4] to measure transmission spectra for μ -mechanical filters with various coupling schemes. Figures 9(a) and 9(b) compare transmission spectra for two MF three-resonator μ -mechanical filters using half- ($\beta=1$) and one-fifth-maximum velocity ($\beta=1.63$) coupling, respectively. As indicated in Table II, even though the filter with half-velocity coupling utilizes more

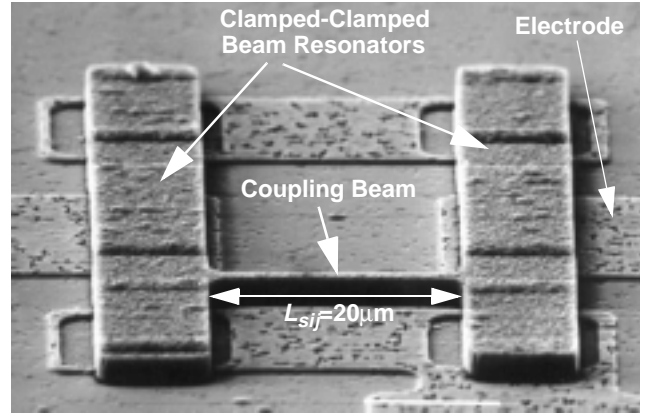


Fig. 8: SEM of a fabricated clamped-clamped beam micromechanical filter

Table II: Micromechanical Filter Design Summary

Parameter	MF Filters		HF Filters	
	$v_{max}/2$ ($\beta=1$)	$v_{max}/5$ ($\beta=1.63$)	$L_r/2$	$L_r/10$
Coupling Location				
Des. BW [Hz]	1000	400	950k	1,300
Meas. BW [Hz]	757	403	340k	1,738
BW/f_o [%]	0.22	0.088	9.5	0.13
m_r [kg]	1×10^{-10}	8×10^{-10}	6×10^{-13}	4×10^{-11}
k_r [N/m]	1,239	6,618	2,347	166,000
L_{sij} [μ m]	74	95	20.4	20.4
W_{sij} [μ m]	1.2	2	0.8	0.8
k_{sij} [N/m]	1.76	3.76	163	163

compliant 1 μ m-wide coupling beams, this filter still exhibits a larger bandwidth (757 Hz, $Q_{fltr}=459$) than its fifth-velocity coupled counterpart, which uses stiffer 2 μ m-wide coupling beams, yet achieves a bandwidth of only 403 Hz ($Q_{fltr}=813$). Furthermore, note from Table II that the fifth-velocity coupled filter was able to closely match the target bandwidth (within 0.75%), unlike its half-velocity counterpart, which missed its target by 24.3%. This result can be attributed to the wider coupling beams of the lower-velocity coupled filter, which are less susceptible to overetch-derived process variations than are the thinner beams of the higher-velocity coupled one. Decreased process susceptibility is, thus, a major advantage afforded by low-velocity coupling strategies.

Figures 10(a) and 10(b) compare transmission spectra for two HF μ -mechanical filters, one with coupling locations at the centers of the resonator beams (maximum velocity coupling), and another with resonators coupled at an anchor-to-location distance equal to one-tenth the length of the resonator beams. Although the bandwidth of the maximum-velocity coupled filter was too large to allow proper termination of the filter [2,4], the difference in bandwidth between the two is clearly seen. However, as seen in

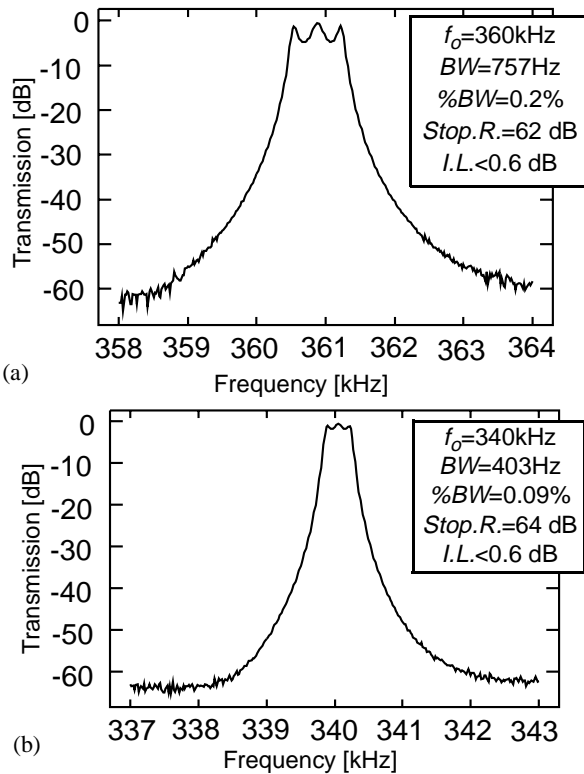


Fig. 9: Measured frequency spectra for low-velocity coupled, folded-beam MF filters. (a) Half-maximum velocity coupled. (b) One-fifth-maximum velocity coupled.

Table II, there are sizable discrepancies between designed and measured bandwidths for the HF filters, irrespective of coupling location. These anomalies can be attributed, first, to process variations (given that both used submicron coupling beam widths), and second, to uncertainty in specifying exact coupling locations due to the finite width of the coupling beams.

It is noteworthy to mention that the measured data in Figs. 9 and 10 illustrate not only the effectiveness of low-velocity design techniques in achieving smaller percent bandwidths with improved accuracy, but also the impressive frequency response performance of μ mechanical filters in general. In particular, Fig. 9(b) shows a filter response with a Q of 813, stopband rejection in excess of 60 dB, and an insertion loss of only 0.6 dB. Such performance rivals that of many macroscopic high- Q filters, including crystal filters, which are some of the best available.

V. CONCLUSIONS

A low-velocity coupling technique has been shown to greatly extend the range of percent bandwidths achievable by surface-micromachined, polysilicon μ mechanical filters operating at both MF and HF frequencies. Using low-velocity coupled designs, filters with minimum feature sizes of $2 \mu\text{m}$ were demonstrated with percent bandwidths of less than 0.1%—a performance mark previously achievable only with submicron coupling beam dimensions. Due to decreased susceptibility to etch-derived planar process vari-

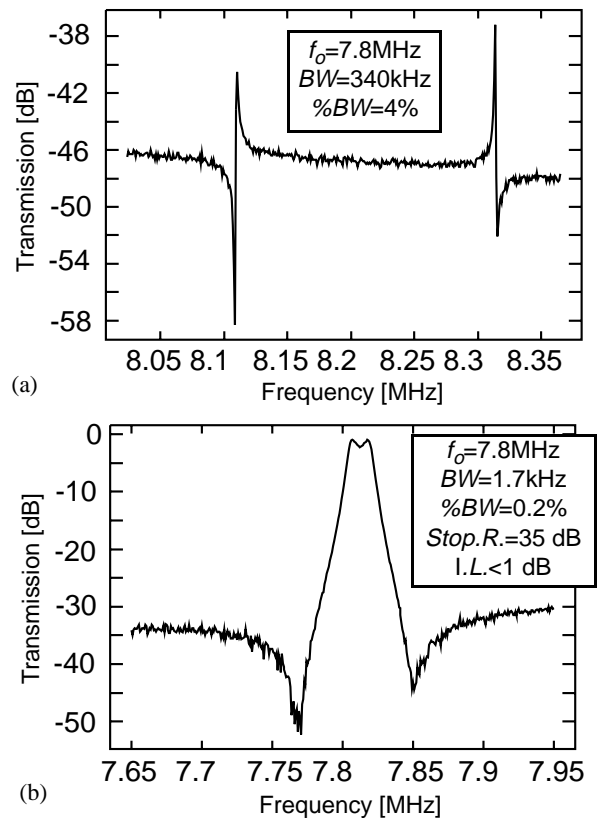


Fig. 10: Measured spectra for clamped-clamped beam HF filters. (a) Maximum velocity coupled. (b) Coupled at one-tenth the resonator beam length.

ations, fabricated low-velocity coupled MF filters were further shown to match designed bandwidth targets better than their high-velocity coupled counterparts. However, discrepancies in designed versus measured bandwidths were still present for HF filters, even after low-velocity coupling. Although these can be attributed largely to process variations, they may also be caused by difficulty in specifying exact coupling locations on clamped-clamped beam resonators by finite width coupling beams. Aside from this, however, low-velocity coupling remains an effective design method for achieving greatly improved bandwidth flexibility and accuracy in micro-scale mechanical filters.

Acknowledgments. This work was supported in part by grants from DARPA, NSF, and the ARO.

References:

- [1] C. T.-C. Nguyen, *ISCAS Proceedings*, pp. 2825-2828, 1997.
- [2] F.D. Bannon, et al., *IEDM Tech. Digest*, pp.773-776, 1996.
- [3] J. R. Clark, et al., *Tech. Digest*, Transducers'97, pp. 1161-1164, 1997.
- [4] K. Wang, et al., *Proceedings*, MEMS'97, pp. 25-30, 1997.
- [5] A.I. Zverev, *Handbook of Filter Synthesis*, 1967.
- [6] R. A. Johnson, *Mechanical Filters in Electronics*, 1983.
- [7] R. T. Howe, et al., *IEEE Trans. Electron Devices*, ED-33, pp. 499-506, 1986.